International Journal of Heat and Mass Transfer 111 (2017) 933–942

Contents lists available at ScienceDirect

International Journal of Heat and Mass Transfer

journal homepage: www.elsevier.com/locate/ijhmt

Evolution and statistics of thermal plumes in tilted turbulent convection

Shuang-Xi Guo, Sheng-Qi Zhou *, Ling Qu, Xian-Rong Cen, Yuan-Zheng Lu

State Key Laboratory of Tropical Oceanography, South China Sea Institute of Oceanology, Chinese Academy of Sciences, Guangzhou 510301, China

ARTICLE INFO

Article history:
Received 5 December 2016
Received in revised form 7 April 2017
Accepted 10 April 2017

Keywords:
Turbulent convection
Thermal plumes
Nusselt number
Plume area density
Plume velocity

ABSTRACT

We present a systematic experimental study of thermal plumes within tilted turbulent thermal convection using the shadowgraph technique. The measurements are performed in a rectangular cell (aspect ratio $\Gamma_x = 1$ and $\Gamma_y = 0.25$) over a wide range of tilt angles ($0 \leqslant \beta \leqslant \pi/2$ rad) at constant Prandtl ($Pr \simeq 10$) and Rayleigh ($Ra \simeq 6.80 \times 10^{10}$) numbers. It is found that the plume width, λ, is distributed log-normally in space and the time-averaged most probable plume width, $\langle \lambda_p \rangle$, has similar scale with the thermal boundary layer thickness, λ_T. $\langle \lambda_p \rangle$ and λ_T slowly increase as tilt angle, β, increases from 0 to 1 rad and they broaden rapidly as $\beta > 1$ rad. The average plume area density, $\langle \Phi \rangle$, deduced from the image intensity, is proposed to represent the heat flux of thermal plumes. Its β dependence is consistent with that of the Nusselt number, Nu, over the tilt angle range. λ_p and Φ exhibit oscillation of convective flow. The oscillation intensity and period strongly depend on β, but are less affected by Ra and Pr. The plume velocity exhibits a different pattern from that of the two-dimensional convective flow measured at $Pr \simeq 6.3$ and $Ra \simeq 4.42 \times 10^9$. The magnitude of plume velocity peak is weakly affected by the cell tilting. The position of the plume velocity peak increases linearly with increasing β.

1. Introduction

Turbulent thermal convection is widely found in nature and industrial applications, e.g., oceanic and atmospheric circulation, planetary convection, and industrial heating or cooling devices. Because of its significance, turbulent thermal convection has attracted much attention and has been extensively studied from theoretical, experimental and numerical approaches based on the classical ideal model, Rayleigh-Bénard convection (RBC). RBC considers a fluid layer in a closed system heated from below and cooled from above, and the convection arises due to fluid buoyancy induced by density differences (for reviews, see Ahlers et al. [1], Lohse and Xia [2], Chillà and Schumacher [3], Xia [4]). In general, the RBC system is determined by three dimensionless parameters, the Rayleigh number $Ra = \alpha g \Delta T H^3/(\nu\kappa)$, Prandtl number $Pr = \nu/\kappa$, and aspect ratio $\Gamma = L/H$, where α is the thermal expansion coefficient, g is gravitational acceleration, ν is kinematic viscosity, κ is molecular thermal diffusivity, ΔT is the temperature difference between the bottom and top conductive plates, H is the cell height, and L is the lateral characteristic length of the cell. Heat transfer efficiency and turbulent dynamics of the convective flow can be denoted with two dimensionless parameters, the Nusselt number $Nu = F_H H/(\chi \Delta T)$ and Reynolds number $Re = UH/\nu$, where F_H is the heat flux of the system, χ is molecular thermal conductivity, and U is a characteristic flow velocity. The main focus of previous research has been how Nu and Re depend on the control parameters, Ra, Pr and Γ [1–4].

There are three main types of coherent structures in RBC, boundary layers, thermal structures (referred to here as thermal plumes), and large scale circulation (LSC) (see, for example, Fig. 1 in Xia [4]). Instability of the boundary layers generates the thermal plumes, which are emitted into the bulk flow randomly and continuously [5]. Interaction between the plumes and LSC leads to initial horizontal motion of the plumes near the boundaries [6], then the plumes merge into clusters and rise or fall near the sidewall [7].

As one of the most important coherent structures, thermal plumes form and drive LSC [6,7], and primarily transfer vertical heat flux [8–10]. The thermal plumes are generally considered to be generated and detached from the boundaries [7,11–14], and occur in sheets or mushrooms. Sheet plumes are mainly close to the conductive plates and convolute into spiraling swirls, then move away from the plates and cluster into mushrooms [14,15]. With increasing distance from the plates, the number of sheet and mushroom plumes decrease and increase, respectively [15], and have a 0.3 scaling exponent with Ra, which is close to the scaling exponent between Nu and Ra [16]. Plume physical properties, such as width, area, perimeter, shape, spatial distribution, and heat content universally follow log-normal distribution [15–17]. Plume

* Corresponding author.
E-mail address: sqzhou@scsio.ac.cn (S.-Q. Zhou).

http://dx.doi.org/10.1016/j.ijheatmasstransfer.2017.04.039
0017-9310/

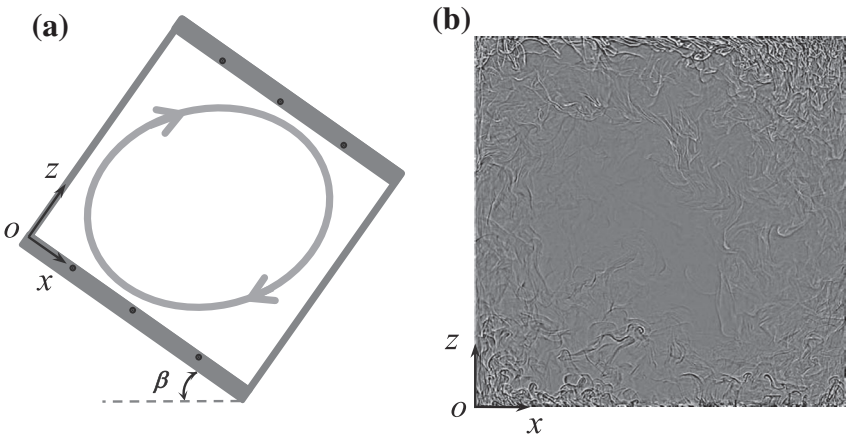

Fig. 1. (a) Schematic diagram of the convection cell with the large scale circulation (LSC) plane (x-z plane). The x and z coordinate axes are along the bottom plate and the sidewall, respectively, and the y coordinate is perpendicular to x and z, with the origin at the bottom left. The coordinate frame moves with the tilt angle β. Six thermistors are inserted into the top and bottom plates, as shown. (b) Shadowgraph image recorded at $\beta = 0.49$ rad. The dark (bright) stripes framed by bright (dark) ones correspond to hot (cold) plumes.

velocity reflects the movement of thermal structures, which may not be the same as flow velocity of fluids. Ching et al. [18] extracted local plume velocity from simultaneous measurements of local velocity and temperature. The thermal plumes can be directly captured using shadowgraph technique (e.g., Xi et al. [6], Funfschilling and Ahlers [10]), which offers an opportunity to evaluate the global plume velocity field in the turbulent convection.

For practical cases, e.g. ocean convection, heat exchangers, etc., the boundary conditions are somewhat more complicated. A particular case of interest is when the heating power is applied at a tilted boundary, as opposed to the horizontal heating boundary in RBC. The effect of cell tilting on heat transport, flow dynamics, and boundary layers with a small tilt angle β (less than 0.2 rad) has been extensively studied. Ciliberto et al. [19] performed experiments in a rectangular cell with $Pr = 3$, $Ra = 10^6$–10^{11}, and $\Gamma = 1$–6. When the cell is tilted by 0.175 rad, they found that the LSC is forced close to the boundary, but the heat transport remains unchanged. Cioni et al. [20] performed a similar experiment in a cylindrical cell with $Pr = 0.025$, $Ra = 5 \times 10^6$–5×10^9, and $\Gamma = 1$. They found the azimuthal motion is confined and LSC reversals are inhibited, but the heat transport changes no more than 1% with cell tilted up to 0.07 rad. Chillà et al. [21] reported a systematic experiment in a cylindrical cell with $Pr = 2$, $Ra \sim 10^{12}$, and $\Gamma = 0.5$. They found heat transport decreases up to 5% when the cell is tilted by 0.03 rad. A similar experiment was performed by Sun et al. [22] in a cylindrical cell with $Pr = 5.3$, $Ra = 5.3 \times 10^{10}$, and $\Gamma = 0.5$. They found a Nu reduction of 2–5% when the cell was tilted by 0.035 rad. Ahlers et al. [23] performed a more comprehensive study in a cylindrical cell with $Pr = 4.38$, $Ra \sim 10^{11}$, and $\Gamma = 1$. They found a slight Nu reduction of 0.5% but significant Re increase of 14% when the cell was tilted up to 0.17 rad. Recently, Weiss and Ahlers [24] observed a slight increase of Nu for tilt angles up to 0.1 rad in a cylindrical cell with $Pr = 4.38$, $Ra \sim 10^{10}$, and $\Gamma = 0.5$. They also found that azimuthal diffusion is suppressed with increasing tilt angle. The small tilt angle has a weak effect on heat transport, which may be the reason for the different scalings between Nu with β in different works [21–26]. The effect of cell tilting on the boundary layer was also explored experimentally for $\beta < 0.06$ rad, and showed that boundary layer thickness has different Ra dependencies at different β [27]. Recently, Guo et al. [26] studied the effect of cell tilting on flow dynamics and heat transport in a rectangular cell over a wide range of tilt angle, $0 \leqslant \beta \leqslant \pi/2$ rad, for $Pr \simeq 6.7$ and $Ra \simeq 4.4 \times 10^9$. They found that Re first increases and then decreases as β increases, with transition at $\beta = 0.15$ rad, which is similar to the experimental and numerical work by Bairi et al. [28], aside from the different transition angles. They also found that cell tilting causes a pronounced reduction of Nu. More recently, Shishkina and Horn [29] numerically investigated the effect of tilt angle, $0 \leqslant \beta \leqslant \pi/2$ rad, on Nu and Re in a cylindrical container with $10^6 \leqslant Ra \leqslant 10^8$, $0.1 \leqslant Pr \leqslant 100$. They found that Nu and Re have distinct and complicated relationships with β, Ra, and Pr. Thus, Nu has a different β dependence from Re, which suggests detailed thermal measurements are required.

To examine the role of thermal plumes in heat transport and flow dynamics of a tilted cell, we take measurement of thermal plumes over a wide range of tilt angles ($0 \leqslant \beta \leqslant \pi/2$ rad) using the shadowgraph technique. Section 2 provides detailed descriptions of the experimental setup, and we present the method and procedures to extract thermal plumes from shadowgraph images in Section 3. The results are discussed in Section 4, focusing on plume width, area density, and velocity. The variances of these plume properties are discussed in the context of global heat transport and convective flow. We summarize and conclude the paper in Section 5.

2. Experimental apparatus and setup

The experimental apparatus includes a light source, rectangular convection cell, high sensitivity thermistors, charge-coupled device (CCD) camera, and multimeter. The convection cell is the same as that used by Guo et al. [26], with length L_x, width L_y and height H being 257, 65 and 257 mm, respectively. The corresponding aspect ratios are $\Gamma_x = L_x/H = 1$ and $\Gamma_y = L_y/H = 0.25$. Since the rotational symmetry of the cell is broken, only one single-roll LSC is confined within the plane of $\Gamma_x = 1$. The top and bottom plates are made of copper with good conductivity (~400 W/mK), and electroplated to avoid corrosion. The sidewall is 9.5 mm thick Plexiglas. The temperature of the top plate is kept constant at 16.35 °C by a refrigerated circulator (Polyscience Model 9702), and an electric heater pad is embedded into the bottom plate and connected to a DC power supply (GE, Model GPS-3030) to provide heating. The temperature of each plate is detected by three embedded thermistors (Fig. 1(a)) and recorded by a digital multimeter (Keithley, Model 2700) with 4 Hz sampling rate. To effectively capture thermal plumes using the shadowgraph technique, silicone oil (Shi-